

Yu.M. Solonin, O.Z. Galiy, A.V. Sameljuk, L.O. Romanowa, K.O. Graivoronska

The Influence of Step-By-Step Air Exposition of the Zr-Mn-Cr-Ni-V Alloy on Cycle Life

Frantsevich Institute for Problems of Material Sciences, NAS Ukraine 3, Krzhyzhanovsky str., Kyiv, 03680, Ukraine

In the course of the research it was determined that step-by-step air exposition of the Zr-Mn-Cr-Ni-V alloy (in the form of ingot and powder) facilitating the formation of concentration inhomogeneity significantly increases the cycle life of electrodes. An electrode compacted of step-by-step exsposed ingot of the alloy demonstrates no loss of capacity during 190 cycles. With the decrease of porosity, caused by adding the nickel powder with significantly smaller particle size than that of particles of the alloy, or by increase of plasticizer content from 5 % to 10 %, the electrodes are being destroyed much sooner due to formation of more dense packing.

Based on the polarization curves of the researched alloy and manganese that demonstrate similar electrochemical behavior in non-oxidized state and stability in oxidized state, the conclusion is made that the increased stability and, as a consequence, the cycle life of the air-exsposed alloy is mainly achieved due to manganese which is stably passive in oxidized state.

Keywords: Zr-alloy, hydrogenation, exposition in air.

Article acted received 23.08.2017; accepted for publication 05.09.2017.

Introduction

Nickel–metal hydride (NiMH) batteries are becoming widespread due to high operating characteristics and environmental safety [1-3]. AB₂ type (Laves phases) zirconium alloys, which properties depend significantly on the component and phase composition, are promising materials for nickel–metal hydride batteries.

One of the basic requirements for metal-hydride electrodes, when they are used in practice, is long cycle life when working in an alkali electrolyte. A reduction of cycle life is possible as a consequence of mechanical destruction due to the significant volume effect of the hydrogenation-dehydrogenation reaction and corrosion. Many methods are used to increase the cycle life of the alloy. One of the methods is the creation of a certain concentration inhomogeneity, thereby reducing the mechanical stresses at the interphase boundaries that leads to a reduction in the formation of cracks and corrosion [4]. It is possible to achieve concentration inhomogeneity in multicomponent zirconium alloys, and to use Ni, Cr, Mn, Co and others as alloying elements.

We have studied the electrochemical properties of a multicomponent zirconium alloy in order to find ways to improve its kinetic and cyclic characteristics and have found a positive effect of air exposition of the alloy on

the indicated characteristics. In further studies, it has been established that a more effective way of improving cycle life is the step-by-step exposition of the alloy (in ingots and in powder). In our opinion, concentration inhomogeneity is also created with step-by-step exposition, that contributes to the increase of cycle life. The results of these studies are presented in this paper.

Since the behavior of alloys of the AB₂ type during hydrogenation-dehydrogenation is highly dependent on the elemental composition, the electrochemical behavior of some of the alloy components and their ability to be in equilibrium with their own ions in the electrolyte, at which achievement further dissolution (corrosion) of the elements does not occur, that affects properties of the alloy as a whole [5] has been studied.

I. Experimental details

The alloy (30 g) was obtained by the argon-arc melting method. The composition of the alloy is given in Table 1.

The alloy samples were validated by X-ray diffraction analysis using DRON-3M with Bragg-Brentano focusing. The voltage and current on the X-ray tube were 30 kV and 25 mA, respectively. The recording was carried out in Cu K α - monochromatic radiation in

Table 1

| Composition of Zr-containing alloy | | | | |
|-------------------------------------|------------|------------|-----------|----------|
| Formula composition | | | | |
| Zr -1 | Mn – 0.5 | Ni – 1.2 | Cr – 0.20 | V – 0.1 |
| Weight % of components in the alloy | | | | |
| Zr – 44.58 | Mn – 13.42 | Ni – 34.43 | Cr – 5.08 | V – 2.49 |

Table 2

| Optimal parameters of the device | | | |
|---|-----------|-----------|----------|
| | Ni | Mn | Cr |
| Lamp current, mA | 4 | 5 | 5 |
| Flame stoichiometry | oxidizing | oxidizing | reducing |
| Wavelength, nm | 232.0 | 279.5 | 257.9 |
| Slit width, nm | 0.2 | 0.2 | 0.2 |
| Optimal operating range of concentrations, g/ml | 0.1-20 | 0.02-5 | 0.06-15 |

the range of angles 2Θ from 30 to 80 degrees with a scanning step of 0.05° , the integral action time was 10 seconds. A single crystal of graphite was used as a monochromator on a secondary beam.

Powder morphology, structure and chemical inhomogeneity of the material were examined by scanning electron microscopy and X-ray microanalysis using the microanalyzer "Superprobe-733" (JEOL, Japan). The morphology was recorded in secondary electrons (SEI), structures were recorded in reflected electrons (BEI). The investigations were carried out with an accelerating voltage of 25 kV and a beam current of 1×10^{-10} A for electron microscopic studies and 2×10^{-7} A for X-ray spectral studies. Working vacuum was 1×10^{-5} atm.

The voltage-current characteristics were studied by the method of potentiodynamic polarization curves from the stationary potential of the electrode to a potential of -1.6V (forward stroke) and from -1.6V to -0.6 V (reverse stroke) relative to the oxide-mercury reference electrode in a three-electrode cell with separated electrode spaces in a 30 % KOH solution using the PI-50-1.1 potentiostat at a potential sweep speed of 2 mV/s.

The cycle life of the samples was studied by cycling in the galvanostatic mode in a two-electrode cell on a 4-channel automatic module equipped with nonvolatile memory, which provides the restoration of experimental data during repeated program launches. The measurements were carried out at a temperature of $20 \pm 2^\circ\text{C}$ in a 30 % solution of KOH. The electrode of the Ni / Ni (OH)₂ system served as the counter electrode. The charge of the electrodes was conducted with a current of 50 mA for 1.5 hours, a discharge with a current of 5 mA until a potential difference of 0.8 V or 1.0 V was reached.

The amount of dissolved components of the alloy

(nickel, manganese, chromium) in KOH was determined by atomic absorption spectroscopy (AAS). The method is based on measuring the degree of absorption of resonance radiation by free metal atoms formed as a result of spraying the analyzed solution in an air-acetylene flame. The relationship between the measured value and the concentration of the assignable element is established during calibration. AAS is one of the most precise methods for determining low concentrations, characterized by high selectivity, sensitivity and speed of execution. The work was performed on an atomic-absorption spectrophotometer AAS-3.

To increase the sensitivity of the determination of the above elements, the optimal parameters of the instrument were selected (Table 2). To eliminate the effect of acids, their concentration in working and calibration solutions was equalized.

II. Results and discussion

According to the X-ray diffraction analysis the main phase component of the investigated ZrMnCrNiV alloy is a cubic phase with MgCu₂ type C₁₅ structure. Along with this phase, there is also a significant amount of hexagonal phase C₁₄ of MgZn₂ type and secondary phases of Zr₇Ni₁₀ and Zr₉Ni₁₁ intermetallic compounds.

For the studies, the electrodes shown in Table 3 were prepared. Electrodes were prepared by cold pressing of particles (less than 100 μm), in a nickel grid (tablet diameter is 8 mm) with additives of polytetrafluoroethylene as a binder. Mass of the alloy in the compressed electrodes was 0.1 g.

Figures 1 and 2 show the results of a study of the cycle life of electrodes compacted from the alloy in ingot previously exposed in air (2 months), followed by its

Table 3

| Electrodes prepared from ZrMnCrNiV alloy powders of different genesis | | | | | |
|--|-------------------------------------|-----------------------------------|---------------------|-----------------------|---------------------------------------|
| Air exposition of the alloy in the form of an ingot (30-40g) for 2 months followed by a step-by-step exposition in powder * | | | | | |
| Electrode № | Exposition time, days | | Amount of binder, % | Addition of nickel, % | Discharge to difference potentials, V |
| | particle size 600-100 μm | particle size < 100 μm | | | |
| 1 | | 6 | 5 | | 0.8 |
| 2 | 3 | 3 | 5 | | 0.8 |
| 3 | 3 | 3 | 5 | | 1.0 |
| 4 | 6 | | 5 | | 0.8 |
| 5 | | 6 | 10 | | 0.8 |
| Air exposition of the alloy in the form of an ingot (30-40g) for 2 months followed by exposition in the form of an ingot weighing 3g for a month | | | | | |
| 6 | | 0 | 5 | | 0.8 |
| 7 | | 0 | 5 | 10 | 0.8 |
| 8 | | 0 | 5 | 50 | 0.8 |
| Air exposition of the alloy in the form of an ingot (30-40g) for 5-6 months followed by exposition in the form of powder | | | | | |
| 9 | | 0 | 5 | | 0.8 |
| 10 | | 7 | 5 | | 0.8 |

* Air exposition of the alloy powder with a particle size of 600-100 μm with further grinding and exposition of the powder with particle size <100 μm

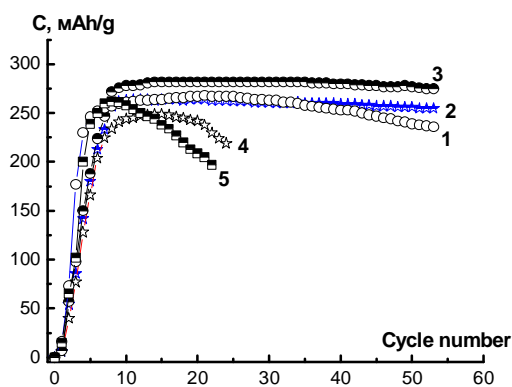


Fig. 1. Dependences of the specific capacity of electrodes № 1-5 on the number of cycles. The number of the curve corresponds to the electrode number according to Table 2.

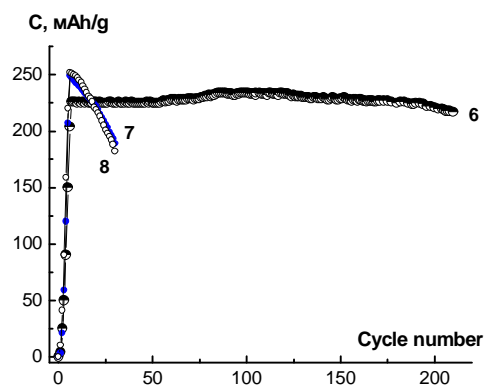


Fig. 2. Dependences of the specific capacity of electrodes № 6-8 on the number of cycles. The number of the curve corresponds to the electrode number according to Table 2.

grinding and additional exposition in powder (Fig. 1, electrodes № 1-5) and ingot (Fig. 2, electrodes № 6-8).

According to Fig. 1, the longest cycle life was shown by electrode № 2 made of the step-by-step air exposed alloy powder (with a particle size of 600-100, followed by its grinding and exposition in a powder with a particle size of 100 μm), in comparison with electrode № 1 compacted from an exposed powder only with a size particles < 100 μm . After 55 cycles loss of capacity of electrode № 2 was 3.3 %, and of electrode № 1 was

12 %. The maximum cycle life had electrode № 3, compacted from the alloy powder step-by-step air exposed, discharged until the potential difference was $E = -1.0 \text{ V}$. For 55 cycles, its loss of capacity was only 2.5 %. Among the electrodes exposed in air during the same time (6 days) but with different particle sizes (electrodes № 1 and 4), the electrode of smaller particles has longer cycle life.

An increase in the binder content from 5 to 10 % (curve 5) in our case does not create a skeleton capable to

prevent the mechanical destruction of the electrode but on the contrary leads to its faster destruction. In our opinion, this is due to the decrease in porosity, which has negative consequences for the mechanical stability of the electrode, which undergoes up to 25 % volumetric expansion under hydrogenation.

A plateau with a length of 190 cycles was obtained on the electrode step-by-step air exposed in the ingot (Fig. 2, curve № 6). The electrode began to lose capacity after 190 cycles of hydrogenation-dehydrogenation as a result of mechanical destruction of the nickel grid and shedding of the material, which was observed visually. Also, nickel powder in the amount of 10 and 50 % (electrodes № 7 and 8) was added to this investigated material. The surface of the compacted alloy powder with particle size < 100 μm without additives and with

additives of nickel powder in an amount of 10 % is shown in Fig. 3. In our case, the addition of nickel powder resulted in complete mechanical destruction of the electrodes. The compacted electrode is 60% composed of particles with a size of 100 – 80 μm, and the added nickel powder, which morphology is shown in Fig. 3 (f), has a particle size of several μm. As a result of the powder addition, the pores were closed with the creation of a denser packing (Figure 3d, e) compared to the electrode without nickel additives (Figs. 3, b, c), so the electrodes № 7 and 8 mechanically failed (Fig. 2, curves 7 and 8). Electrodes № 5, 7 and 8 clearly demonstrate the effect of porosity on cycle life. To detect nickel particles and their distribution in the material, a recording of the surface area in the reflected electrons and in the Ni_{kα} characteristic X-ray radiation was carried

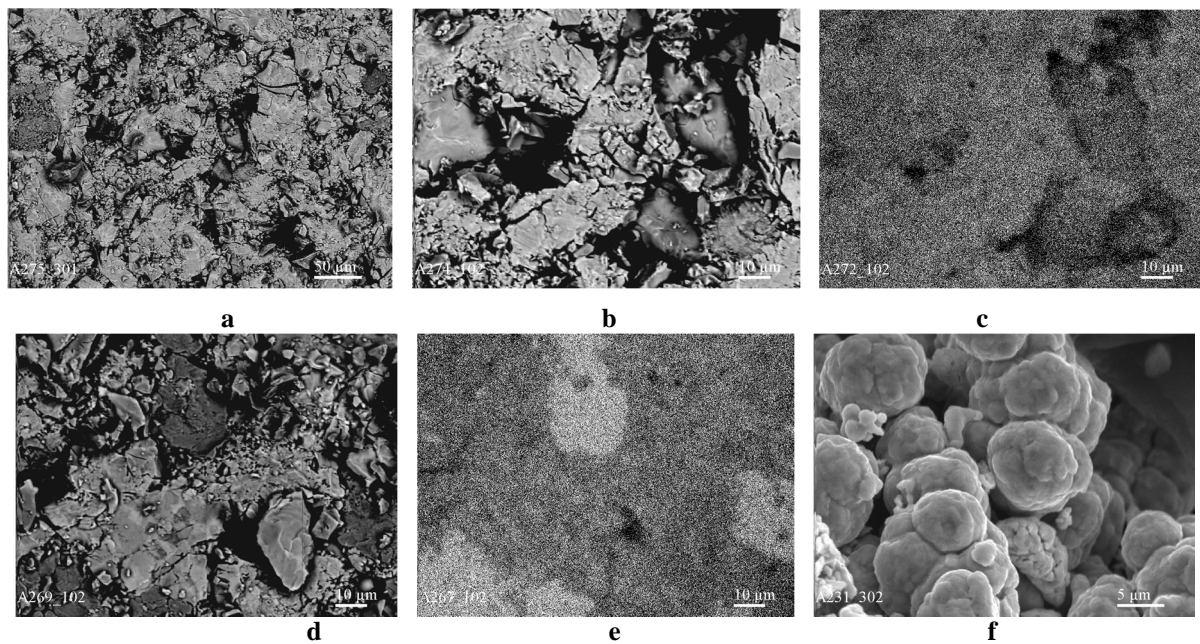


Fig. 3. The surface of the compacted powder of the alloy with particle size < 100 μm without additives (a-x300 BEI, b-x1000 BEI, c-x1000 X-Ray Ni_{kα}) and with additives of nickel powder in an amount of 10 % (d-x1000 BEI, e-x1000 X-Ray Ni_{kα}), f- nickel powder, x3000SEI.

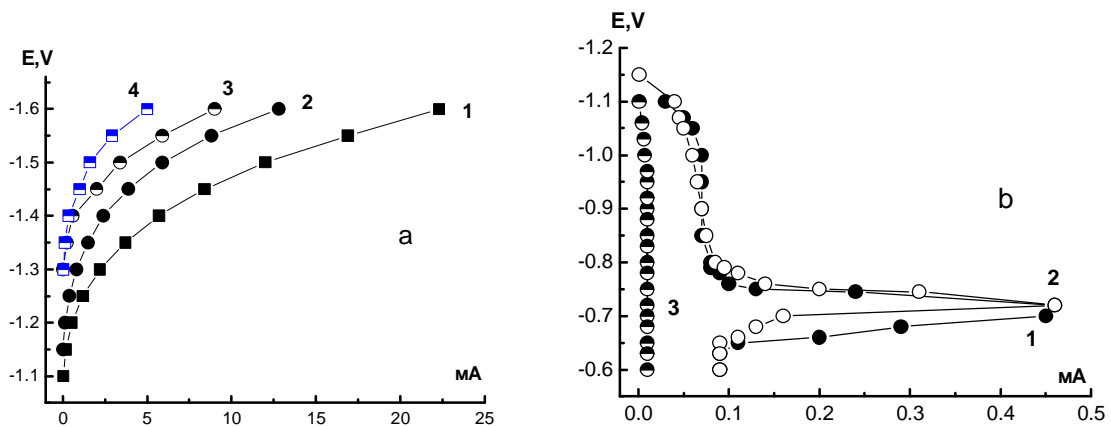


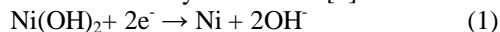
Fig. 4. The cathodic (a, forward stroke) and anodic (b) polarization curves of potentiodynamic cycling of electrolytic manganese without exposition (1-4 (a), 1-2 (b)) and exposition in air for 5-6 months in the form of an ingot (3 (b)); 1-4 (a), 1-3 (b) is the number of the cycle; 4 - after aging the tablet for 30 minutes in KOH solution.

out. In Fig. 3, e, the bright sections correspond to the nickel; in Fig. 3, d, they are darker, since its atomic number is lower than the average atomic number of the alloy.

Since each component of the alloy affects its surface or bulk properties, the electrochemical behavior of the unexposed (initial) and exposed for 5-6 months (in the form of a plate) of electrolytic manganese and nickel powder stored in air for several years, the content of which in alloy is 13.42 and 34.43 %, respectively. The manganese stored in the air for a long time was reduced in a vacuum electric furnace SNV, and then the reduced manganese was exposed in the air for 5-6 months. Figures 4 and 5 show cathodic (forward stroke) and anodic polarization curves of manganese and nickel powders pressed into a nickel grid (tablet diameter is 8 mm) with mass of 0.1 g.

Analysis of the curves in Figures 4a and 5a shows that the manganese unexposed in air loses its activity in the cathode region faster than the nickel powder stored for several years in air (curves 1, 2 and 3 in Figs. 4a and 5a, respectively). After aging in a solution of KOH for 30 minutes, it is practically passive, and the activity of

nickel after similar aging in solution is greater in almost the whole investigated region of potentials than in the first 3 cycles (curve 4 in Figures 4a and 5a, respectively). In the anodic region, nickel retains its activity (Fig. 5, b), while manganese is active only in its original form (Fig. 4b, curve 1-2), and after exposition in air manganese is completely passive (Fig. 4, b, curve 3). In the potential region $E = -0.72$ V (Fig. 4, b and 5, b, curves 1 and 2), where there is a sharp increase in the anode current followed by passivation, in addition to the oxidation reaction of absorbed hydrogen, oxidizing processes occur. Taking into account the electrochemical behavior of manganese exposed in air (Fig. 4, b, curve 3) the manganese oxidation reaction dominates over the electroreduction reaction in this range of potentials that leads to its complete passivity. Electrochemical behavior of nickel indicates that it is capable to be oxidized and reduced according to reaction (1) in contrast to manganese. A similar behavior of nickel (the ability of $Ni(OH)_2$ to be reduced to metallic Ni during battery charging) is also claimed by the authors [6].



Earlier we carried out polarization studies of the

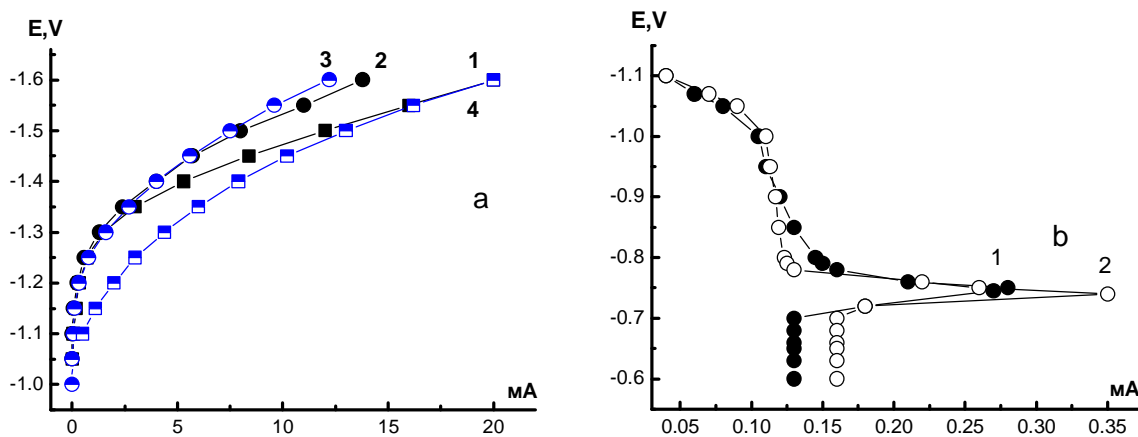


Fig. 5. Cathodic (a, forward stroke) and anodic (b) polarization curves of potentiodynamic cycling of nickel powder after its storage in air for several years; 1-4 (a), 1-2 (b) - the number of the cycle; 4 - after aging the tablet for 30 minutes in KOH solution.

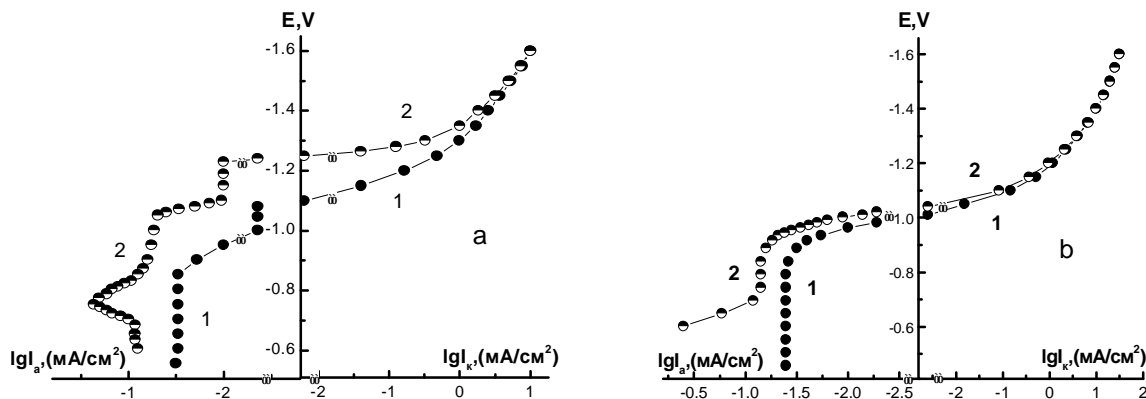


Fig. 6. Cathodic and anodic polarization curves of electrodes: a - № 9, b - №10. The number of the electrode corresponds to the number according to Table 2. 1- forward stroke, 2- reverse stroke.

electrodes made of the unexposed (initial) alloy and freshly melted alloy exposed in air for 7 days, for which an abrupt increase of current to $I_a = 66$ mA in the potential region $E = -0.72$ V was observed in the anodic region. After a long exposition of the alloy (in the form of an ingot) (the results of its study are shown in Fig. 6 (a, b)) the electrochemical processes stabilize, as a result electrode № 9 has a small current increase in the same potential region up to $I_a = 22$ mA (Fig. 6a, curve 2), and electrode № 10 do not have this increase. In this case, the cathodic curves of the forward and reverse stroke of cycling of electrode № 10 almost completely coincide.

A joint analysis of Figures 4, 5, 6 and the previous study of the electrochemical properties of the freshly melted alloy shows the same behavior of the alloy and manganese, namely, the presence of peaks on the anodic curves in the potential region $E = -0.72$ V for the initial alloy and manganese, and the absence of peaks after air storage for 5-6 months. In nickel, after long-term air storage, the peak in the indicated potential region is present.

Thus, as a result of air exposition of the alloy cycle life increased (Fig. 7) that is largely promoted by manganese, which is stably passive in the oxidized state. The question arises concerning the positive effect of the presence of manganese in it as an alloying element on the cycle life of the alloy (if "yes", then in what quantity). The alloying element during hydrogenation-dehydrogenation loses its activity, which, in turn, is accompanied by electrochemical transformations, stresses and, as a result, mechanical destruction of the electrodes.

To evaluate the ability of the alloy components to be in equilibrium with their own ions in the electrolyte, two

30 % KOH solutions of 5 and 20 ml volume were investigated, in which 0.3 g of an alloy powder with a particle size < 100 μm air aged during a month was aged during 45 days. Ni, Mn, Cr high-purity metals were used to calibrate the spectrophotometer. Several calibration solutions (corresponding to the optimal measurement interval) were prepared by gradually diluting the relatively concentrated initial solutions (Fig. 8). Calibration curves, which have linear character and are in the region of the determined concentrations, were plotted using the measured values of adsorption of standard solutions.

From the decanted initial solutions with a volume of 5 ml. (№ 1) and 20 ml (№ 2) (Table 4) aliquots (a) were taken. Their alkaline medium was neutralized, then brought to an acidic using mixture of sulfuric (1:1) and nitrate (1:1) acids and diluted to a volume of 25 ml with distilled water. The concentration (α) of nickel, chromium and manganese in these solutions was measured using a spectrophotometer and recalculated for initial (c).

According to the data given in Table 4, the number of nickel ions transferred to solutions of 5 ml and 20 ml (ratio 1:4) is the same and is $3.5 \cdot 10^{-5}$ g, which corresponds to 7.8 and 1.9 $\mu\text{g} / \text{ml}$ (ratio 4: 1). It follows from this that the dissolution of nickel does not depend on the volume of the electrolyte, but is a function of time. In 5 ml of electrolyte chromium was not found, and in 20 ml of electrolyte its concentration is greater than that of nickel and is $5.7 \cdot 10^{-5}$ g, that is most likely due to the fact that the corroded nickel is mainly on the surface of the alloy in the form of NiO and Ni (OH)₂ with low electrical conductivity [7]. The absence of chromium in 5 ml of electrolyte indicates its very low concentrations

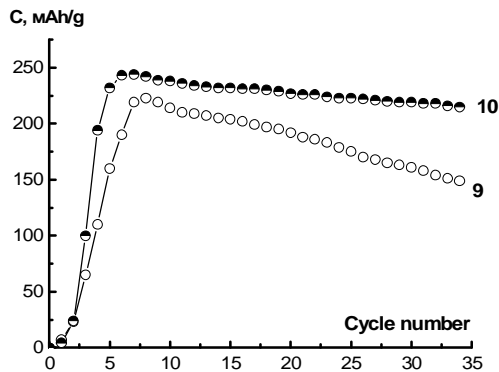


Fig. 7. Dependences of the specific capacity of electrodes №. 9-10 on the number of cycles. The number of the curve corresponds to the electrode number according to Table 2.

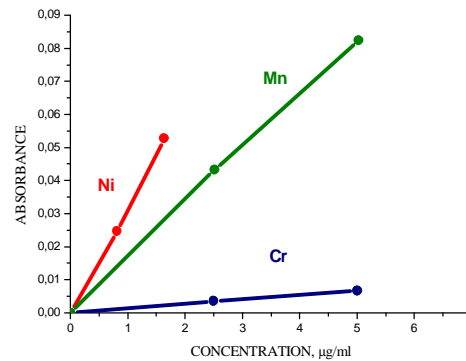


Fig. 8 Calibration curves of nickel, manganese and chromium.

Table 4

Concentration of nickel and chromium in electrolyte solution

| № | a, ml. | Ni | | | Cr | | |
|---|--------|--------------------------------|------------------------------------|---------------------|--------------------------------|------------------------------------|---------------------|
| | | $C_w, \mu\text{g} / \text{ml}$ | $C_{in.}, \mu\text{g} / \text{ml}$ | m, g. | $C_w, \mu\text{g} / \text{ml}$ | $C_{in.}, \mu\text{g} / \text{ml}$ | m, g. |
| 1 | 2 | 0.625 | 7.8 | $3.5 \cdot 10^{-5}$ | | $< 2^*$ | --- |
| 2 | 10 | 0.755 | 1.9 | $3.5 \cdot 10^{-5}$ | 1.24 | 3.1 | $5.7 \cdot 10^{-5}$ |

* The minimum chromium concentration that a device can determine is 2 $\mu\text{g} / \text{ml}$

that cannot be determined and that chromium is capable, as contrasted to nickel, dissolve before equilibrium with its own ions in the solution, after which the loss of mass of the alloy due to dissolution (corrosion) of chromium does not occur. Corroded manganese in the solutions studied is not found, which means that it is located on the surface of the alloy forming non-conductive oxide layers.

Studies on the effect of manganese on the cycle life of the alloy and the results of atomic absorption spectroscopy are well combined with the literature data. Thus, the authors of [8, 9] investigated the alloy Ti-Zr-V-Mn-Ni, gradually replacing manganese with iron, aluminum, cobalt and chromium [8], and in [9] only chromium. The results of these studies show that in the case of the replacement of manganese by chromium, the cycle life of the alloy increases in proportion to the decrease in the amount of substituted manganese, which is explainable on the basis of our studies.

Conclusions

Thus, it was established that the step-by-step air exposition of the alloy (in the form of an ingot and in a powder) promotes a significant increase of the cycle life of the electrodes. When the porosity is reduced (due to the addition of nickel powder with a particle size much smaller than the alloy particles or due to an increase in the amount of plasticizer from 5 to 10 %), the electrodes are rapidly destroyed due to the formation of a more dense packing.

The components of the alloy manganese and nickel show different electrochemical behavior. Manganese,

both during hydrogenation-dehydrogenation and air exposition for 5-6 months, loses its activity until complete passivity. Nickel, stored in air for several years, has the ability in the range of working potentials of the electrode to oxidize and reduce. The investigated alloy and manganese exhibit the same electrochemical behavior, namely, the presence of peaks on the anodic curves in the region of the potential $E = -0.72$ V in the initial form and the absence of peaks after their storage in air for 5-6 months, which indicates stabilization of the properties. In nickel, after storage in air, a peak in the indicated potential region is present. The air exposed alloy shows increased stability and, as a consequence, increased cycle life, that to a large degree promoted by manganese, which is stably passive in the oxidized state. At the same time, according to the analysis by the method of atomic absorption spectroscopy (AAS) corroded manganese is located on the surface of the alloy forming non-conductive oxide layers that is negative for hydrogenation.

Solonin Yu.M. - academician, professor, doctor of physical and mathematical sciences, director of IPM NAS of Ukraine,

Galiy O.Z. - Junior Research Fellow;

Sameljuk A.V. - Researcher;

Romanova L.O. - senior researcher, candidate of chemical sciences;

Graivoronska K.O. Senior Researcher, PhD in Physics and Mathematics.

- [1] I.P. Jain, J. Hydrogen Energy 34, 7368 (2009).
- [2] Yu. M. Solonin, L.L. Kolomiets, V.V. Skorokhod, Sorbent alloys for Ni-MH current sources (Academy of Sciences of Ukraine, Frantsevich Institute for Problems of Material Sciences, Kiev, 1993).
- [3] B.E. Paton, ICHMS-2001, Proceedings of the 7th International Conference on Hydrides (Alushta, 2001). P. 11
- [4] J.J.G. Willems, K.H.J. Bushow, J. Less-Common Met. 129(1), 13 (1987).
- [5] N.P. Beetle, Course on corrosion and metal protection (Metallurgy, Moscow, 1968).
- [6] Z.P. Li, B.H. Liu, K. Hitaka, S. Suda, J. Alloys and compounds 330-332, 776 (2002).
- [7] S.L. Medway, C.A. Lucas, A. Kowal, R.Y. Nichols, D. Yoncn, J. Electroanal. Chem. 587(1), 172 (2006).
- [8] Y.F. Zhu, H.G. Pan, G.Y. Wang, M.X. Gao, J.X. Ma, C.P. Chen, Q.D. Wang, J. Hydrogen Energy 26, 807 (2001).
- [9] G.Y. Wang; Y.H. Xu, H.G. Pan, Q.D. Wang, J. Hydrogen Energy 28, 499 (2003).

Ю.М. Солонін, О.З. Галій, А.В. Самелюк, Л.О. Романова, К.О. Грайворонська

Вплив постадійної експозиції на повітрі сплаву Zr-Mn-Cr-Ni-V на циклічну стійкість

Інститут проблем матеріалознавства ім. І.М. Францевича НАН України, 3, вул. Кржижановського, Київ, 03680, Україна, e-mail: o.galiy87@gmail.com

В ході проведених досліджень встановлено, що постадійне експонування сплаву Zr-Mn-Cr-Ni-V на повітрі (в формі злитка і в порошок), що сприяє створенню концентраційної неоднорідності, істотно підвищує циклічну стійкість електродів. Електрод, спресований з поетапно експонованого сплаву у формі злитка, протягом 190 циклів не має втрат ємності. При зменшенні пористості (шляхом добавок порошку нікелю з розміром частинок значно меншим, ніж частинки сплаву, або збільшення вмісту пластифікатора з 5 до 10 %) електроди значно швидше руйнуються внаслідок створення більш щільної упаковки.

На підставі поляризаційних кривих досліджуваного сплаву і марганцю, які показують однакову електрохімічну поведінку в неокисленому і стабільність в окисленому стані, зроблено висновок, що підвищена стабільність і, як наслідок, циклічна стійкість експонованого на повітрі сплаву багато в чому досягається завдяки марганцю, стабільно пасивному в окисленому стані.

Ключові слова: Zr-сплав, гідрування, експозиція на повітрі.